

**S. Sunil Kumar
K. Ramamurthi**

Propulsion Research and Studies Group,
Liquid Propulsion System Centre,
Trivandrum,
India 695547

Influence of Flatness and Waviness of Rough Surfaces on Surface Contact Conductance

The effect of surface roughness, waviness and flatness deviations on thermal contact conductance is predicted. Threshold values of the surface parameters which do not adversely influence thermal contact conductance are determined. Flatness deviations less than ten times the average roughness and waviness less than about four times the average roughness do not significantly affect the contact conductance. A correlation is developed for contact conductance in terms of the surface parameters, the material properties and the contact pressure at the joint. Experiments are conducted in vacuum with rough, non-flat and wavy surfaces and the experimental results are demonstrated to agree well with the predictions. [DOI: 10.1115/1.1565093]

Keywords: Contact Resistance, Heat Transfer, Roughness, Thermal, Wavy

Introduction

A large number of theoretical and experimental studies have been carried out to estimate the thermal surface contact conductance between joints formed by rough but conforming flat surfaces [1–5]. A surface is characterized not only by the roughness but also by its flatness and waviness. The influence of the flatness and waviness of surfaces on the contact conductance has not been rigorously analyzed, partly due to difficulty of describing the three dimensional topography of surface flatness and waviness in a physical model. The importance of maintaining flat surfaces at the joint has, however, been recognized [1]. Deviations in flatness and waviness would depend on the speed of machining the surface, the depth of cut and the hardware material. The emergence of modern machining techniques makes it possible to achieve high levels of surface finish, flatness and non-waviness since the feed and depth of cut are controlled within a few microns. It is, however, far from clear whether very high levels of surface flatness and waviness, such as can be generated by the advanced manufacturing processes, are necessary to give good surface contact conductance especially when the characteristic surface roughness is typically of the order of a few microns.

Clausing and Chao [1] have suggested that the deviations in the flatness can be accounted for by means of a “spherical cap” model. Here, the apparent contact area is divided into a non-contact region that contains few or no microscopic contact areas and a contact region where the density of micro contacts is high. The flow of heat is constrained in the model to the large scale contact areas. The macroscopic constriction was seen to have a significant influence on the conductance.

Yovanovich [6] extended the theory of Clausing and Chao [1] to predict the conductance of rough wavy surfaces. The macroscopic contact areas were termed as “contour areas.” The study, however, did not quantify the explicit influence of waviness or deviations in flatness on thermal contact conductance.

Thomas and Sayles [7] characterized a surface as comprising of a continuous spectrum of wavelengths. The largest wavelengths with large amplitude deviations, corresponding to large-scale errors of form, were termed as flatness deviations. Smaller wavelengths were taken to constitute the waviness. The smallest waviness represented the roughness. The thermal contact conductance was shown to be proportional to $P^{1/3}$ where P is the contact pres-

sure when the surface is characterized by waviness alone. Similar results were obtained by Madhusudana [8]. If surface roughness is the only consideration, the conductance would be proportional to $P^{0.94}$ [8]. It may be noted that the majority of experimental results obtained with different materials in contact show the exponent of the contact pressure to be between these two values of 1/3 and 0.94. Madhusudana [9] observed the flatness deviations to be important at low contact pressures even when the magnitudes of the deviations are comparable to mean surface roughness.

A detailed review of the different models and their predictions of thermal contact conductance of metallic surfaces carried out by Lambert and Fletcher [10] showed that most of the empirical and semi-empirical correlations have very limited applicability when contacting surfaces are wavy and non-flat. Marotta et al. [11] used a thermo-mechanical model that combined both microscopic and macroscopic thermal resistances. A macroscopic thermal constriction resistance from Hertzian contact theory was employed after due modifications for rough surfaces.

Lambert and Fletcher [12] in a recent work modified a semi-empirical model developed by Mikic [13] for non-flat rough metal surfaces and employed it to predict the conductance of metallic coated surfaces. They considered the distribution of pressure in the contact region. The predictions were demonstrated to compare well with experimental data.

Machining techniques have advanced to a level wherein high degree of surface finish can be achieved. Inspection procedures using stylus based and non-contact measurements can also measure the high degree of surface finish. The requirement for the cost-intensive high accuracy machining and the inspection procedures to ascertain the surface finish cannot be justified if their contribution to improve the thermal contact at the joints is not substantial. It is the intention of the present study to determine the effect of waviness and flatness deviation on otherwise conforming rough surfaces and to determine whether there exist threshold values of surface parameters below which thermal contact conductance is not significantly influenced. The surface characteristics are theoretically modeled, their contact conductance predicted and experiments conducted to verify the predictions.

Theoretical Formulation

Energy transfer across a pressed contact occurs by radiation and conduction through interstitial medium and by conduction through micro-contacts. At relatively low temperatures and pressures, the heat transfer across pressed contacts would be dominated by conduction through actual contact area. Convection would be negli-

Contributed by the Heat Transfer Division for publication in the JOURNAL OF HEAT TRANSFER. Manuscript received by the Heat Transfer Division March 19, 2002; revision received December 5, 2002. Associate Editor: G. Chen.

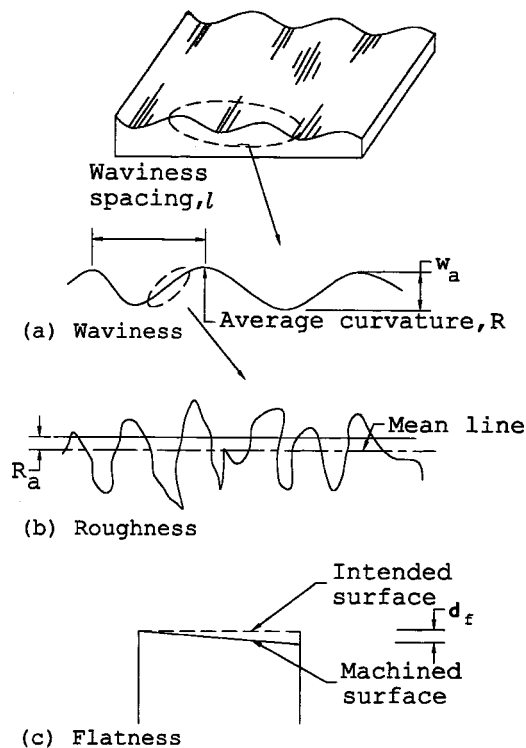


Fig. 1 Representation of surface characteristics

gible for small interfacial clearances, especially at low ambient pressures. In order to model the heat transfer, the contact between the surfaces at the joint needs to be determined. The modeling for the surface contact is given below and is followed by the modelling for the thermal contact conductance.

Model for Surface Roughness, Flatness, and Waviness. A magnified schematic view of a machined surface is shown in Fig. 1. The distribution of asperities is usually not random, but exhibits a preferred direction or lay [6]. The lay contributes to surface waviness. The waviness is represented by the peak to valley height of the measured profile from which roughness is removed by suitable filtering and is represented by an average value w_a [14] (Fig. 1). The average distance between the peaks is represented by waviness spacing length, l . The average curvature of the waviness peak is denoted by R [14,15]. A single value of spacing and curvature is generally used to characterize waviness. Sengupta and Lekoudis [16] use such a description to represent wavy surfaces in their studies of flow in boundary layer. The average surface roughness in Fig. 1 is quantified by a roughness parameter, R_a which is the average height of the profile above and below a mean line as shown. Flatness is defined [15] as the departure of the surface from true flatness and is represented as the maximum deviation of the machined plane from the intended plane. In the particular case of two surfaces under consideration, the deviation d_f corresponds to the sum of deviation obtained for the two mating surfaces and this is schematically shown in Fig. 1. The measurement of the deviation is given subsequently. The modelling of each of these three surface parameters is outlined below.

(a) Surface Roughness. The interaction of asperities from the two rough surfaces leads to individual microscopic contacts at a joint. The modelling comprises of estimating the contact area and is dealt with by Sunil Kumar and Ramamurthi [5]. The surface roughness is described by a standard deviation of combined height distribution (σ) and an average absolute slope (m) for the asperities. The distribution of the asperity heights is assumed to be Gaussian, viz.,

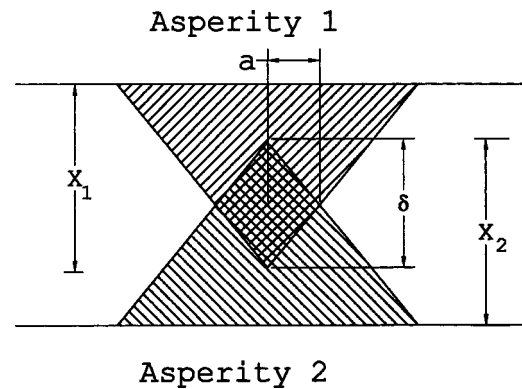


Fig. 2 Physical model of a single asperity contact

$$f(x) = \frac{1}{\sqrt{2\pi}\sigma} \exp\left[-\frac{1}{2}\left(\frac{x-R_a}{\sigma}\right)^2\right] \quad (1)$$

Here $f(x)$ denotes the distribution of asperity heights. The asperity height distribution leads to the determination of the number of asperities per unit area and their height [4] as given below. The number of asperities per unit area is determined as:

$$N = (m/7.308\sigma)^2 \quad (2)$$

The maximum summit height is:

$$x_{\max} = 8\sigma \quad (3)$$

The mean summit height is given by:

$$R_a = 4\sigma \quad (4)$$

The maximum and mean summit heights and the number of asperities per unit area are used to model the actual area of contact for non-flat wavy surfaces as detailed in reference [5]. When two opposing asperities come into contact with each other, as shown in Fig. 2, the asperity summit undergoes a plastic deformation. A contact spot radii, a is formed and is given by:

$$a = 0 \quad \text{if} \quad \delta \leq 0 \quad (5a)$$

$$a = \delta/2m \quad \text{if} \quad \delta > 0 \quad (5b)$$

Here δ is the summit penetration depth and is sketched in Fig. 2. A value of δ less than zero implies that the two asperities are not in contact.

The separation distance or clearance between the reference planes of the two conforming rough surfaces is given by [8]:

$$\varepsilon = \sqrt{2}\sigma \operatorname{erfc}^{-1}\left[\frac{2P_j}{P_j + H}\right] \quad (6)$$

The above expression for clearance takes into account the material hardness (H), the surface roughness (σ) and the contact pressure (P_j) in the contact zone. For conforming flat surfaces, the pressure term in Eq. (6) corresponds to the overall contact pressure based on the apparent area of contact. However, for non-flat surfaces, the pressure would vary in the different contact zones. The contact region is therefore subdivided into large number of elemental areas within which the pressure is assumed to be same. This is dealt with subsequently.

(b) Flatness. The deviation in flatness reduces the macroscopic contact region over and above the reduction caused by the microscopic asperity contact. Figure 3 illustrates the modeling procedure of the contact region for two surfaces A and B . The surface A has a high degree of flatness, whereas B has a flatness deviation of d_f . Only part of the surface facing each other comes into contact as represented by the shaded region shown in Fig. 3(b). This area is referred as the contour area of contact (A_f)

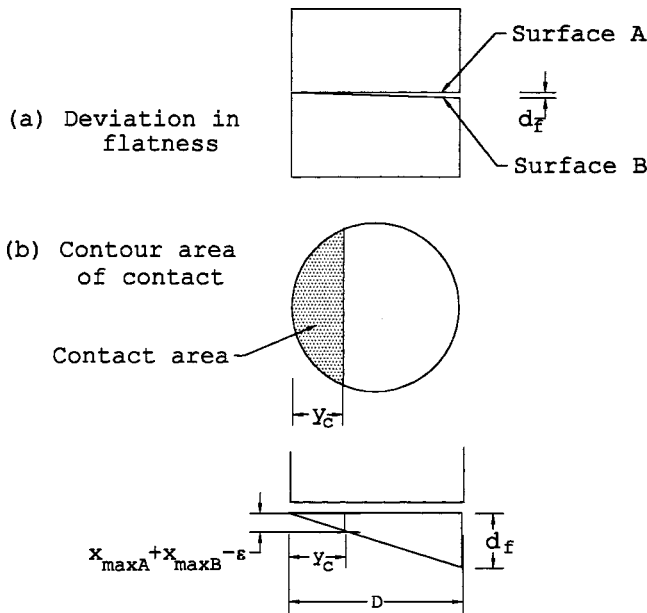


Fig. 3 Physical representation of non-flat rough contact

formed due to flatness deviation [11]. The area would change as the clearance between the contacting surfaces changes. A simple two-dimensional geometrical representation of the surfaces, shown in Fig. 3(b), is used to determine the extent y_c over which the surfaces are in contact. This is given by:

$$\frac{y_c}{D} = \frac{x_{\max A} + x_{\max B} - \varepsilon_{\min}}{d_f} \quad (7)$$

Here $x_{\max A}$ and $x_{\max B}$ represent the maximum asperity height of surface A and surface B, respectively. D is the diameter of the surface. The above expression assumes that the surfaces are in contact up to a limit wherein their respective surface asperities can touch each other. The contact area will depend on the applied pressure. In order to determine the contact area and its variation with pressure, the surface is divided into a number of zones of width dy as illustrated in Fig. 4. The maximum pressure and therefore the minimum clearance (ε_{\min}) would occur at zone $j=1$ for a

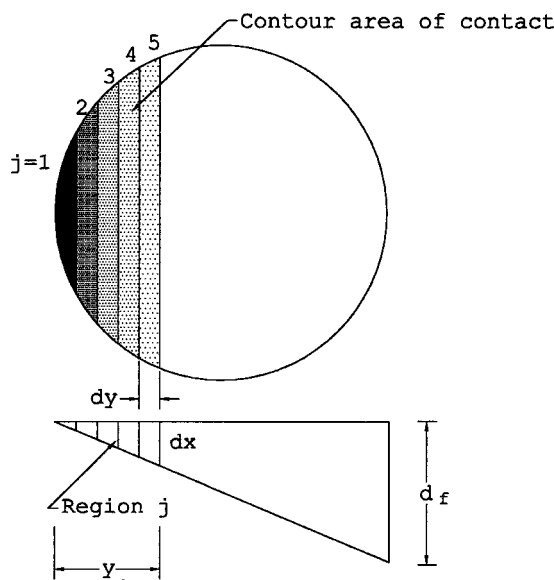


Fig. 4 Descretization of the contact zone

given applied load. The pressure at this zone could be approximated as the ratio of the load to the elemental area. The pressure in each zone will vary along y_c . The pressure is considered to be constant in each of the elemental zones. Knowing the maximum pressure at zone $j=1$, the pressure at subsequent elements is deduced from the following expression [17].

$$P_j = P_1 \left[1 - \left(\frac{j \times dy}{y_c} \right)^2 \right]^{1/2} \quad (8)$$

Here P_1 corresponds to the pressure at zone $j=1$. The width dy of the element is so chosen that the estimated total contact area does not differ more than 2% when the width is halved. The zone $j=1$ is in contact when a small value of pressure is applied at the interface. As pressure is increased additional zones get into contact. The number density of contacting asperities in zone $j=1$ are higher compared to new zones which come into contact as applied pressure is increased. The additional clearance (dx_j) at the boundaries of each discretized zone is given by:

$$dx_j = 1/2[j \cdot dy \cdot df / D + (j+1) dy \cdot df / D] \quad (9)$$

The separation distance is enhanced by the above magnitude over that estimated for rough but conforming flat surfaces. The net clearance for a rough non-flat surface is given by:

$$\varepsilon_j = \varepsilon_{\min} + dx_j \quad (10)$$

(c) **Waviness.** The waviness is quantified in terms of the average waviness height w_a , average spacing l , and average slope or curvature of (R). The macro contact zone of two wavy surfaces could either be in the zones of their respective peaks or between the peaks and valleys. The former would give a small macro contact area whereas the latter would provide substantially larger contact. A large number of combinations of peak and valley contact between the surfaces are theoretically feasible. For joints prepared by turning in a lathe, peak to valley contact at the interface is not probable considering the changes of the depth in the azimuthal direction. The contact zone with waviness is modelled as the sum of the contour area of each contacting waviness peak based on the two-dimensional representation of average waviness height, spacing and curvature. The clearances between the wavy surfaces in contact are determined based on averages unlike in the case of roughness and flatness deviations. The width of the contact zone (w) when two peaks of radii if curvature R_1 and R_2 meet is given by Hertzian contact theory [17] as:

$$w = \left[\frac{3 \pi (K_1 + K_2)}{2 \left(\frac{1}{R_1} + \frac{1}{R_2} \right)} P \right]^{1/3} \quad (11)$$

where,

$$K_1 = \frac{1 - \nu_1^2}{\pi E_1} \quad \text{and} \quad K_2 = \frac{1 - \nu_2^2}{\pi E_2} \quad (12)$$

R_1 and R_2 are macro parameters and the material properties which influence the deformation are the Young's modulus (E) and Poisson's ratio (ν). The contour contact area is found for each of the contacting waviness peaks. The microscopic contact region within this macro area is determined using the roughness parameter (R_a) detailed earlier.

The number of wavy peaks (n_f) in contact is determined from measured values of waviness and flatness parameters. The extent y_c over which the surfaces are in contact is based on waviness height and not on the maximum asperity heights.

Model for Thermal Contact Conductance. The heat flow is constrained at macro level through the contour zones corresponding to the macro constrictions from non-planarity and waviness before being further constrained through the individual micro contacts. In addition to the microscopic constriction resistance (R_s) there are therefore two additional macroscopic constriction resis-

tances [6,7] (R_f and R_w) formed by the area contours due to waviness and flatness deviation. The total constriction resistance (R_t) is therefore given by:

$$R_t = R_s + R_f + R_w \quad (13)$$

The total contact conductance h_t is determined as:

$$h_t = 1/R_t A_a \quad (14)$$

The resistance due to surface roughness (R_s) is determined following Mikic [2] using two flat conforming rough surfaces. The heat flow rate for each individual contact is written as,

$$Q_i = 2ka_i \Delta T_c / \psi_{si} \quad (15)$$

Here ΔT_c is the temperature drop across the interface. The individual constriction alleviation parameter ψ_{si} in the above equation is defined by:

$$\psi_{si} = (1 - (P_j/H)^{1/2})^{1.5} \quad (16)$$

The constriction parameter is considered to be same ($\psi_s = \psi_{si}$) for all contacting asperities in an elemental zone following [4]. If there are n_c contacting asperities over an apparent area A_a , the total heat flow across the joint is given as:

$$Q = \sum_{i=1}^{n_c} Q_i = \frac{2k \Delta T_c}{\psi_s} \sum_{i=1}^{n_c} a_i \quad (17)$$

The thermal contact resistance due to surface roughness alone can be calculated from the above equation as:

$$R_s = \frac{\Delta T_c}{Q} = \frac{\psi_s}{2k \sum_{i=1}^{n_c} a_i} \quad (18)$$

Here n_c represents the number of contacting asperities, a_i is the radius of each individual contact circle formed by the two contacting asperities (Fig. 2) and k is the harmonic mean of the conductivities of the two contacting materials. The values of a_i are obtained from the surface roughness parameter using Monte-Carlo simulation of contacting asperities and is detailed in Reference [5].

The macro resistances due to flatness deviation and waviness (R_f and R_w) is written following [8] as:

$$R_f = \frac{\psi_f}{2ka_f} \quad (19)$$

and

$$R_w = \frac{\psi_w}{2ka_w} \quad (20)$$

The macroscopic constriction parameters ψ_f and ψ_w in the above equation are estimated using the expression developed by Roess [11] which gives:

$$\psi_{f,w} = 1 - 1.4093(x_{f,w}) + 0.2959(x_{f,w})^3 + 0.0525(x_{f,w})^5 \quad (21)$$

where

$$x_f = \frac{a_f}{r_a} \quad \text{and} \quad x_w = \frac{a_w}{r_a} \quad (22)$$

Here, a_f and a_w represent the equivalent radius of the contour area formed respectively by flatness deviation and waviness. r_a is the radius of the apparent area of contact. The total contact conductance can be written from Eq. (14) as:

$$h_t = \frac{1}{\left[\frac{\psi_s}{2k \sum_{i=1}^{n_c} a_i} + \frac{\psi_f}{2ka_f} + \frac{\psi_w}{2ka_w} \right] A_a} \quad (23)$$

Contact Area Due to Roughness, Waviness, and Deviation in Flatness

The number of contacting asperities (n_c) within the macro contact zone and their respective contact spot radii, a_i are determined using Monte-Carlo simulation technique [5]. For two contacting surfaces of a given surface texture, the number of asperities in a discretised contact zone of area A_j is given following Eq. (2) as:

$$N_j = NA_j \quad (24)$$

If $x_{\max 1}$ and $x_{\max 2}$ are the respective maximum asperity heights due to roughness of surfaces 1 and 2, respectively, and if one asperity each is randomly chosen on either surface of height x_1 and x_2 then:

$$\frac{x_1}{x_{\max 1}} \leq 1 \quad \text{and} \quad \frac{x_2}{x_{\max 2}} \leq 1 \quad (25)$$

The individual asperity heights could be assumed to follow Gaussian distribution, and the above equation can be re-written as:

$$\frac{x_1}{x_{\max 1}} \leq U_{x1} \quad \text{and} \quad \frac{x_2}{x_{\max 2}} \leq U_{x2} \quad (26)$$

Here U_x represents Gaussian random numbers between 0 and 1. By randomly assigning values to U_{x1} and U_{x2} , the individual asperity heights can be estimated. If the combined height of the asperities is larger than the clearance, ε calculated earlier for a region j by Eq. (10), then these asperities will touch each other.

The penetration depth of the asperity is given by;

$$\delta = x_1 + x_2 - \varepsilon_j \quad (27)$$

Here ε_j is the clearance for the discretized zone j and considers the cumulative effect of roughness, deviations in flatness and waviness. Once δ is known, the spot contact radii, a_i can be calculated from Eq. (5) derived earlier. The analysis is repeated for all the asperities in all the discretised zones and covers the entire asperities in the contact region. The total number of contact spots (n_c) and their respective contact radii are thus determined.

Predicted Results and Discussions

The micro and macro contact areas derived in the last section are substituted in Eqs. (18, 19, and 20) to determine micro constriction resistance R_s and macro constriction resistance R_f and R_w . The total surface contact conductance is determined from Eq. (23). A flow chart for the computation is given in Fig. 5. A Microsoft Fortran uniform random number generator subroutine RANDOM is used for generating Gaussian random numbers. The subroutine returns a value between 0 and 1 for an input seed value. For the same input seed value repeated computations reproduced results within 0.23%. When the number of random numbers used for the generation of Gaussian random number was doubled, the deviations were found to reduce further. The estimated conductance values differed only by 0.16% between double precision and single precision computations.

The random model was validated by predicting the results for the limiting case of conforming flat and non-wavy surfaces i.e.; $w_a = 0$ and $d_f = 0$. Predictions were done for varying surface roughness and pressure for different materials. The results are compared in Fig. 6 with those obtained for flat surface joints given in Reference [5] as dimensionless contact conductance h^* and pressure P^* . It is seen that almost identical values are obtained over a wide range of contact pressures confirming the basic model to be valid. A large number of computations were carried out by

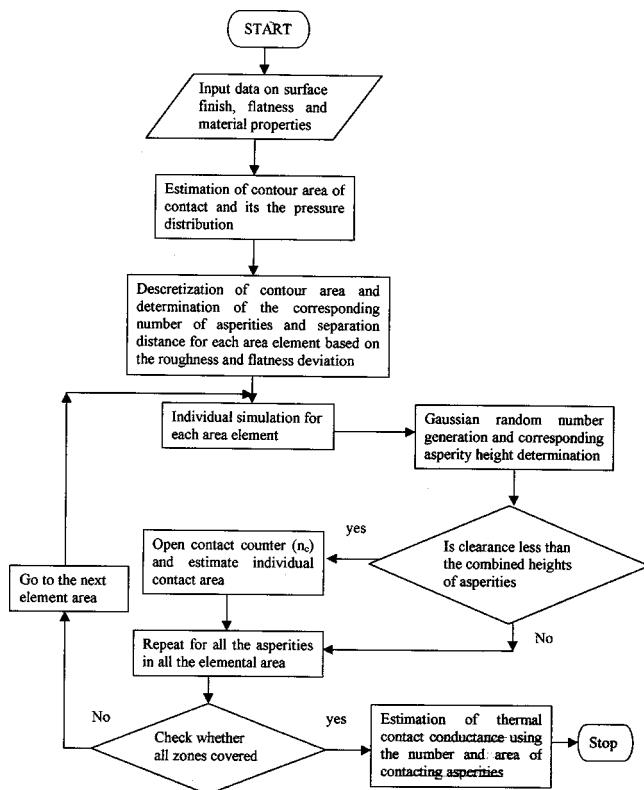


Fig. 5 Computational flow diagram

varying the values of surface parameters, interfacial contact pressure and materials of contacting surfaces. The predictions are discussed below.

Influence of Flatness Deviations. A typical result showing the reduction in actual contact area for a stainless steel joint due to deviation in flatness is illustrated in a log-log plot in Fig. 7 for two different values of contact pressures of 3MPa and 10MPa. The surface roughness parameter, R_a considered is $1.0 \mu\text{m}$. It can be seen that higher contact area persists when the ratio of the flatness deviation to average roughness, (d_f/R_a) is less than about 10. For values of the ratio greater than about 10, rapid decrease of the

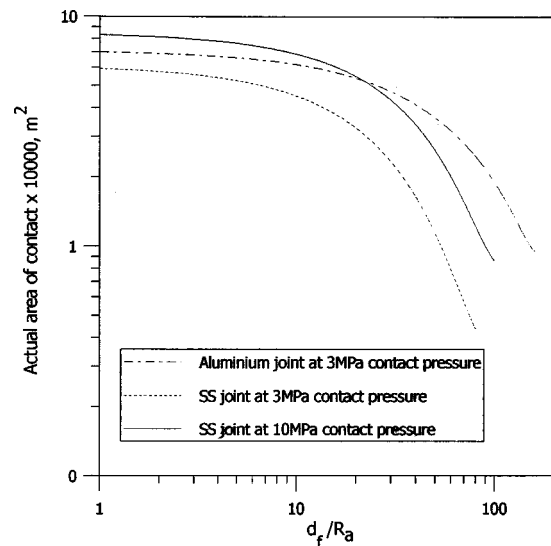


Fig. 7 Effect of flatness deviation on actual area of contact for stainless steel and aluminum joints

contact area is observed. It is also noted from the figure that a higher contact pressure yields higher contact surface area and this is to be anticipated.

A second set of predictions, carried out for an aluminum/aluminum joint at 3MPa contact pressure yielded similar trends and is also included in Fig. 7. The chain-dotted line shows the predictions. For the softer material, the contact area is large and is less influenced by deviation in the flatness.

The variation of contact conductance with changes in flatness is shown in Fig. 8 for aluminum/aluminum joint at a contact pressure of 3MPa. The results are qualitatively similar to the changes in contact area and the conductance values are seen to be higher for lower degree of flatness deviation. As the deviation in flatness increases, the number of contact spots reduces resulting in lower values of thermal contact conductance. There exists a region of $d_f/R_a \leq 10$ wherein the contact conductance values remains fairly unaffected by the changes in flatness. The results suggest that for two surfaces in contact with each other, it is adequate to maintain the surface flatness deviations within approximately 10 times the

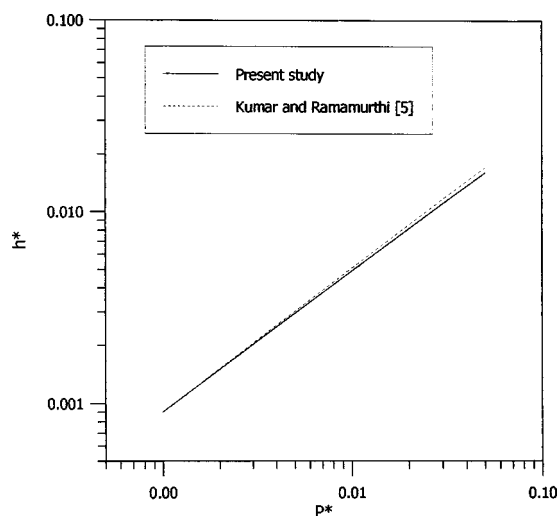


Fig. 6 Comparison with earlier literature for non-wavy flat surfaces

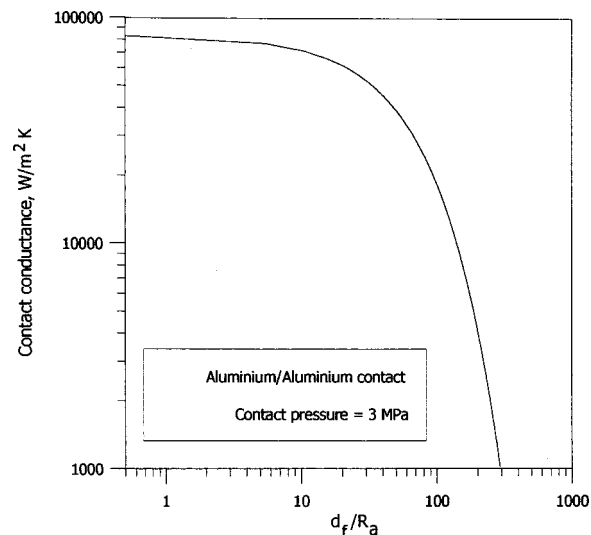


Fig. 8 Influence flatness deviations on thermal contact conductance

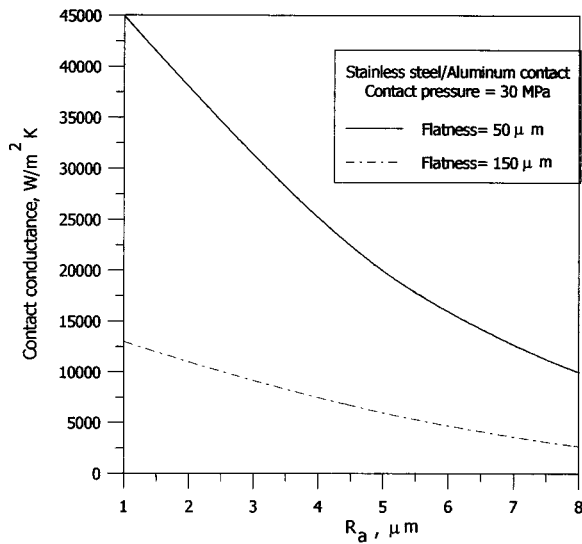


Fig. 9 Inter-dependence of flatness and mean surface roughness

average surface roughness values in order to achieve good thermal contact conductance. Extremely high levels of flatness do not significantly contribute to improvement of the thermal contact conductance.

The variation of the estimated contact conductance values when the average surface roughness is varied for two values of flatness deviations of 50 μm and 150 μm is shown in Fig. 9. Very significant changes in contact conductance values are observed with changes in roughness for the surface having lower flatness deviation. When the magnitude of flatness deviations are comparable with that of surface roughness, the later would influence the contact area and hence affect the values of thermal contact conductance. Flatness deviations of 50 μm and 150 μm , considered in Fig. 9 are very much higher than surface roughness parameter R_a . As the surface roughness parameter R_a increases, the difference in the conductance values between the two non-flat surfaces becomes smaller. For large values of surface roughness, the influence of flatness deviation on thermal contact conductance is small.

Influence of Waviness. The influence of waviness on thermal contact conductance is shown in Fig. 10. A stainless steel/aluminum joint with varying waviness heights for a specified

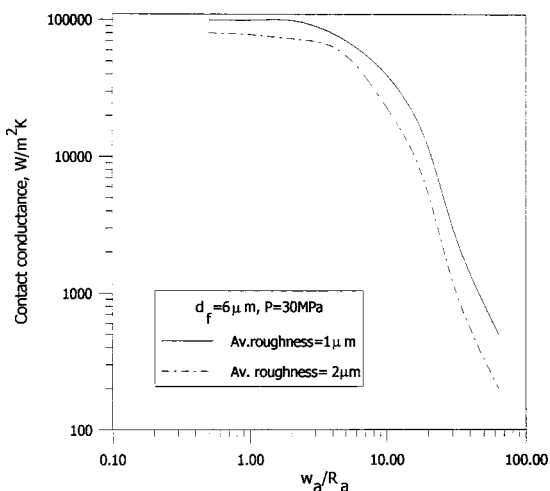


Fig. 10 Surface waviness influence on thermal contact conductance

waviness spacing of 80 μm and an average radius of curvature for wavy peaks of 3 μm is considered. This corresponds to specimens obtained by machining in a conventional lathe. A constant value of surface flatness deviation of 6 μm and an overall contact pressure of 30 MPa is assumed. Two sets of data are shown in the figure corresponding to surface roughness (R_a) values of 1 μm and 2 μm . The thermal contact conductance is seen to be relatively unaffected by changes in the value of waviness of about 4 times the average roughness. This value is much smaller compared to the value of 10 obtained in the case of flatness. Though, flatness is the larger macro surface parameter compared to waviness, the contact conductance at a joint is more strongly influenced by waviness. The stronger dependence is attributed to the large decrease in contact area with increasing waviness heights for a specified value of waviness spacing.

Generalized Results. A large number of predictions of the contact conductance were carried out by varying the surface roughness, R_a , waviness height, w_a and flatness deviation, d_f at different contact pressures for different materials. These predictions were fitted by general correlation which would bring out the relative influence of each of the variables on the thermal contact conductance. Such a correlation could be useful for a designer to fix acceptable limits for the surface finish, waviness, and flatness deviations. The regression analysis procedure of using a dimensionless pressure and contact conductance term [5] in addition to a newly introduced non-dimensional term, K was followed to fit the predicted values. The term K considered the influence of roughness, waviness, and flatness deviations. A least square fit of the results gives the following:

$$h^* = 0.14(P^*)^{0.61}e^{-1/K} \quad (28)$$

where

$$h^* = \frac{h\sigma}{mk}; \quad P^* = \frac{P}{H}; \quad \text{and} \quad K = 3.8\sigma \left(\frac{2}{d_f + \frac{w_a l}{R_{av}}} \right) \quad (29)$$

Here, R_{av} denotes the harmonic mean of the average curvatures of the waviness peaks of the two surfaces. The above correlation is valid over the range of dimensionless loading parameter between 0.0014 and 0.1. The value of K is varied between 0.13 and 5. The standard error in the h^* estimate is 0.0074. The exponent of pressure load is found to be 0.61 which is very close to the values reported by Leung et al. [4], Sunil Kumar and Ramamurthi [5] and Madhusudana [8]. The additional term, K has a negative exponent and brings down the value of contact conductance. The macro surface properties are therefore important. For the limiting case of non-wavy conforming flat surfaces (w_a and d_f tending to very small values), close match is seen between the present correlation and that reported in reference [5].

Experiments

Test Specimen. Stainless steel and aluminum rods 7 cm long and 3 cm in diameter were used for the experiments. These two materials were chosen as they are widely used in different applications and their mechanical and thermal properties are well known. Rough surfaces with flatness deviation were prepared in a conventional milling machine. The preparation of wavy surfaces was more involved and a lathe was programmed for the movement of the cutting tool at speeds between 0.3 mm/rev and 1.8 mm/rev.

The surface finish, waviness, and flatness deviations of the surfaces were evaluated from two-dimensional measurements of surface topography. A Form Talysurf with digital readout facility which uses a position sensitive variable inductance transducer was used to measure the surface characteristics. The transducer converts the small vertical movements of a diamond stylus into proportional variation of electrical signal. The transducer had a sen-

Table 1 Details of test specimens

Test pair	Specimen	R_a (μm)	d_f (μm)	w_a (μm)	l (μm)
1	SS 304	1.3	17	—	—
2	Aluminum	1.5	17	—	—
3	SS 304	0.6	10	4	980
4	Aluminum	0.6	10	3	700

sitivity of $0.01 \mu\text{m}$. Surface roughness and waviness were determined over an evaluation length of 2.5 cm. The signals obtained over the evaluation length were analyzed for cut-off length as per International Standards Organization (ISO). The cut-off length is the minimum length required to give valid measurement of microscopic irregularities. A cut off length of 0.8 mm was chosen for turned surfaces [14]. The distribution of surface heights determined within the cut-off length corresponded to surface roughness and gave the roughness profile. The average surface roughness R_a was obtained the measurements over the entire evaluation length.

The waviness was determined by filtering the roughness from the profile obtained over the evaluation length. The macroscopic undulations obtained after the filtering constitute the waviness and were fitted in the Talydata-2000 software for average surface parameters w_a , l , and R . The above representation of waviness using averages for depth, spacing and curvature is done following the procedure of Dagnall [14].

The flatness deviation d_f of each surface is obtained by filtering out the surface roughness and waviness in the Talysurf measurements. The instrument had a measurement accuracy of $\pm 2\%$ over the specified range of 0 to $20 \mu\text{m}$.

A total of 8 test specimens, 4 each of stainless steel and aluminum were made. The range of surface finish, waviness and flatness deviations in the specimen is given in Table 1 given below. The ratio of d_f/R_a varied between 13 and 16 and the ratio w_a/R_a varied between 5 to 6.7 in the specimens. These values are seen from the prediction to be in the region where waviness and flatness do influence the contact conductance.

Experimental Setup. The surface contact conductance was measured in an axial heat flow apparatus. A sketch of the test apparatus is shown in Fig. 11. Test coupons were heated by a heat flux standard (heater). These standards generate a specified value of one-dimensional heat flux. The power input to the heat flux standard was controlled by a variac and measured through a precision digital wattmeter. The contact pressure at the interface was varied by tightening the loading bolt. A load cell placed between the heater and the loading bolt was used for the measurements. The contact pressure was varied between 5 MPa and 70 MPa.

An insulator (Fig. 11) was used to reduce the heat transferred through the loading bolt. The insulator was made out of Vespel, a material possessing an extremely low thermal conductivity ($\approx 0.02 \text{ W/mK}$). Six thermocouple junctions of T -type were at-

tached to the surface of the test specimen 7 mm apart. The thermocouples were welded to the test specimen using a discharge type thermocouple welding machine. The load cell and thermocouple outputs were connected to a Fluke Hydra series digital multimeter (DMM) with scanner.

The set-up was placed inside the vacuum chamber of approximately 180 litres capacity. Vacuum was achieved using a two-stage rotary vane vacuum pump. The level of vacuum was measured using a Pirani gauge with readout facility. All experiments were conducted at vacuum better than 10^{-3} mbar. A heat flux gauge was placed below the bottom sample, as shown in Fig. 11, to assess the heat transfer rate through the sink.

The heat flow through the specimen was maintained at about 5.0 watts for the experiments. The thermal path through the specimen showed a much smaller thermal resistance than the thermal path through the pointed loading bolt. The heat transfer through the specimen was determined with the measured temperature gradients. These values were about the same as the power input to the heater indicating that transverse and upward heat flow through the loading mechanism were negligibly small. The radiation loss to the surrounding was minimized by covering the test pieces by a bright aluminum foil. The maximum value of the measured total heat loss was within 9%.

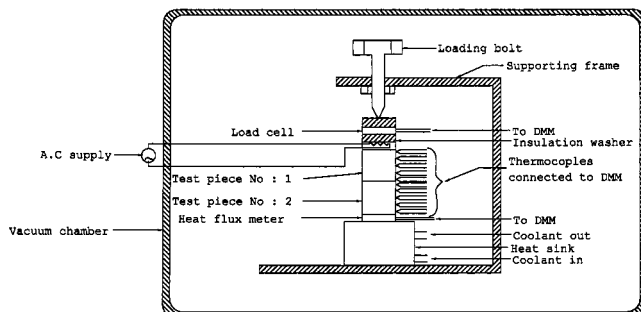
The assumption of steady state was taken to correspond to a situation when maximum temperature change over a period of 5 minutes was less than 0.1°C . In practice, steady state conditions were reached within 40 minutes. However, for the first set of experiments involving initiation from cold conditions, the transients were much longer (almost 190 minutes).

Uncertainty in Measurements. A key factor affecting contact heat transfer measurements is the heat loss. The heat loss was ensured to be small by maintaining the resistance of heat flow to the surrounding to be sufficiently large compared to the contact resistance at the interface. Since the experiments were done in a vacuum chamber, the major source of heat loss to the surrounding is by radiation. The measurement of the temperature differences and the error in locating the thermocouples also contributed to the uncertainties in measurement. All the thermocouples were fabricated in the laboratory and were calibrated using high accuracy microprocessor-controlled temperature bath with an accuracy of $\pm 0.1^\circ\text{C}$ prior to use. The interfacial temperature difference in the experiments varied between 2°C and 18°C and the mean interfacial temperature varied from 50°C to 73°C .

The maximum uncertainty is associated with experiments having highest load across the joint and for specimens of smoothest surface having least surface waviness and flatness deviations. This condition results in the smallest temperature drop across the interface. The maximum uncertainty in the differential temperature measurement is $\pm 0.3^\circ\text{C}$ for the smallest temperature difference of 2°C and corresponds to 15% uncertainty. With heat conduction through the specimens known within 9%, the largest uncertainty in measured thermal contact conductance was therefore $[0.09^2 + 0.15^2]^{0.5} = 17.5\%$. The accuracy of measurements was much better for wavy and non-flat surfaces and for test coupons with larger values of surface roughness. The pressure and load measurements were accurate within 2% of the nominal.

Experimental Results and Comparison. Experiments were first done for non-flat and non-wavy surface contacts formed by stainless steel joints and aluminum joints and then repeated with wavy and non-flat surfaces given in Table 1. All experiments were carried at different values of interface contact pressures. Figure 12 gives a comparison of the measured values with the values obtained from prediction and from the generalized correlation given by Eq. (28).

The measured values are seen to be in excellent agreement with the predictions and the correlation. Higher values of contact conductance for aluminum/aluminum contact is to be anticipated due to its lower material hardness. Under pressure, aluminum flows

**Fig. 11 Experimental set-up**

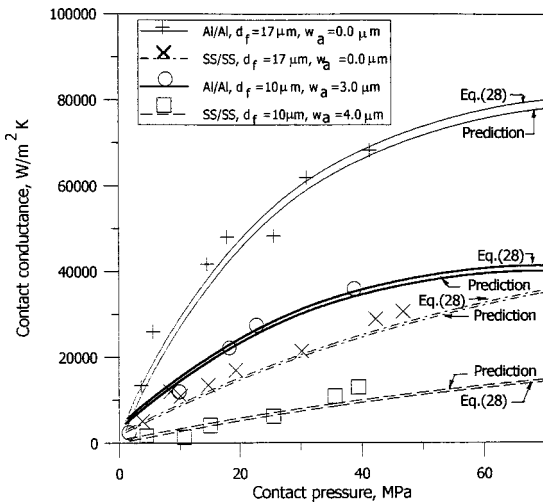


Fig. 12 Comparison of experimental results with predictions and generalized correlation

easier leading to higher values of contact area and hence the contact conductance. A few points in both aluminum and stainless steel joints show deviations which are well within the measurement accuracy of the experiments. Waviness drastically brings down the contact conductance in both stainless steel and aluminum samples confirming that waviness is indeed a very strong surface parameter in the determination of contact conductance. For wavy samples at lower contact pressures, the measured values were observed to be lower than predictions. This could be attributed to the assumption of perfect peak to peak contact in the model. The correlation matches with most of the experimental data within 17%.

Conclusions

The influence of the roughness, waviness and flatness of surfaces on contact conductance is determined. The macro contact area corresponding to deviation in flatness and waviness and the micro contact area for surface roughness is modeled and the surface contact conductance predicted. Experiments are also done with stainless steel and aluminum samples having different levels of waviness, flatness and roughness. The results of the experiments are demonstrated to match closely with the theoretical predictions.

The surface waviness is observed to influence surface contact conductance more strongly compared to flatness deviations. Deviation in flatness less than about 10 times the surface roughness and waviness less than about 4 times the surface roughness do not strongly influence the thermal contact conductance. Flatness is the larger macro surface parameter compared to waviness and the contact conductance is consequently less strongly influenced by waviness. The influence of waviness and flatness is particularly pronounced at smaller values of contact pressures and for harder materials of construction.

A generalized correlation is developed for contact conductance to include the effect of surface roughness, waviness and flatness deviations. The influence of contact pressures and material properties are included in the correlation. The correlation matches with the experimental results within about 17%.

Acknowledgment

The authors thank Mr. Abhilash, P.M for the assistance in conducting the experiments. The helpful discussions with Professor C.V. Madhusudana of University of New South Wales are grate-

fully acknowledged. The comments and suggestions of the anonymous reviewers helped in revising the manuscript. Their suggestions are also acknowledged.

Nomenclature

- a = radius of contact spot/contour, m
- A = area, m²
- D = diameter of the sample, m
- d_f = deviation in flatness, μm
- E = Young's modulus, Pa
- h_t = total thermal contact conductance, W/m²K
- h^* = dimensionless contact conductance
- H = micro hardness of the softer material, Pa
- j = number of the discretized region
- K = dimensionless surface parameter
- k = harmonic mean of thermal conductivities, W/mK
- l = waviness spacing, μm
- m = slope of the asperity
- N = density of asperities, per m²
- n = number of contacting asperities
- P = overall contact pressure, Pa
- P_j = contact pressure for zone j , Pa
- P^* = dimensionless pressure
- Q = heat flow rate, W
- R = radius of curvature of waviness peak, m
- R_a = mean surface roughness, μm
- $R_{f,s,w,t}$ = resistance due to flatness, roughness, waviness and total, K/W
- ΔT = temperature difference
- U_x = Gaussian random number
- w = width of area of contacting wavy peaks, m
- w_a = average waviness height, μm
- x = summit heights, m
- δ = summit penetration depth, m
- ε = clearance between the surfaces, m
- ν = Poisson's ratio
- σ = standard deviation in summit heights, m
- $\psi_{f,s,w}$ = constriction alleviation factor due to flatness, roughness, and waviness

Subscripts

- a = apparent
- av = average
- c = asperity contact
- i = i th asperity
- j = j th discretized region
- max = maximum
- r = real
- w = contour contacts due to waviness
- $1,2$ = surfaces 1 and 2

References

- [1] Clausing, A. M., and Chao, B. T., 1965, "Thermal Contact Resistance in Vacuum Environment," *ASME J. Heat Transfer*, **87**, pp. 243–251.
- [2] Mikic, B. B., 1974, "Thermal Contact Conductance; Theoretical Considerations," *Int. J. Heat Mass Transf.*, **17**, pp. 205–214.
- [3] McWaid, T., and Marschall, E., 1992, "Thermal Contact Resistance Across Pressed Metal Contacts In Vacuum Environment," *Int. J. Heat Mass Transf.*, **35**, pp. 2911–2920.
- [4] Leung, M., Hsieh, C. K., and Goswami, D. Y., 1998, "Prediction of Thermal Contact Conductance in Vacuum by Statistical Mechanics," *ASME J. Heat Transfer*, **120**, pp. 51–57.
- [5] Sunil Kumar, S., and Ramamurthi, K., 2001, "Prediction Of Thermal Contact Conductance In Vacuum Using Monte-Carlo Simulation," *J. Thermophys. Heat Transfer*, **15**, pp. 27–33.
- [6] Yovanovich, M. M., 1969, "Overall Constriction Resistance Between Contacting Rough, Wavy Walls," *Int. J. Heat Mass Transf.*, **12**, pp. 1517–1520.
- [7] Thomas, T. R., and Sayles, R. S., 1975, "Random Process Analysis Of The Effect Of Waviness On Thermal Contact Resistance," *Prog. Astronaut. Aeronaut.*, **39**, pp. 3–20.
- [8] Madhusudana, C. V., 1996, *Thermal Contact Conductance*, Mechanical Engineering Series, Springer-Verlag, New York, pp. 35.
- [9] Madhusudana, C. V., 2000, "Accuracy In Thermal Contact Conductance

- Experiments—The Effect Of Heat Losses To The Surroundings,” Int. Commun. Heat Mass Transfer, **27**, pp. 877–891.
- [10] Lambert, M. A., and Fletcher, L. S., 1996, “A Review Of Thermal Contact Conductance Of Metals,” AIAA Paper 96-0239.
- [11] Marotta, E. E., and Fletcher, L. S., 2001, “Thermal Contact Resistance Models Of Non-Flat, Roughened Surfaces With Non-Metallic Coatings,” ASME J. Heat Transfer, **123**, pp. 11–23.
- [12] Lambert, M. A., and Fletcher, L. S., 2002, “Thermal Contact Conductance Of Non-Flat, Rough, Metallic Coated Metals,” ASME J. Heat Transfer, **124**, pp. 405–412.
- [13] Mikic, B., 1970, “Thermal Constriction Resistance Due To Non-Uniform Surface Conditions; Contact Resistance At Non-Uniform Interface Pressure,” Int. J. Heat Mass Transf., **13**, pp. 1497–1500.
- [14] Dagnall, H., 1986, *Explaining Surface Texture*, Rank Taylor Hobson Ltd., UK
- [15] Whitehouse, D. J., 1994, *Handbook of Surface Metrology*, IOP Ltd, UK, Chap. 2.
- [16] Sengupta, T. K., and Lekoudis, S. G., 1985, “Calculation of Turbulent Boundary Layer Over Moving Wavy Surfaces,” AIAA J., **23**(4), pp. 530–536.
- [17] Seely, F. B., and Smith, J. O., 1963, *Advances in Mechanics of Materials*, Wiley, NY, Chap. 11.